"Icebergs" or No "Icebergs" in Aqueous Alcohols?: Composition-Dependent Mixing Schemes

Yoshikata Koga,*,†,‡ Keiko Nishikawa,§ and Peter Westh‡

[1]Department of Chemistry, The University of British Columbia, Vancouver, British Columbia, Canada V6T 1Z1, Department of Biological Sciences and Chemistry, Roskilde University, Roskilde DK-4000, Denmark, Graduate School of Science and Technology, Chiba University, Chiba 263-8522, Japan

Received: November 26, 2003; In Final Form: February 10, 2004

The classical concept of "iceberg formation" is modified by our recent thermodynamic studies. The local enhancement of the hydrogen-bond network of H_2O in the immediate vicinity of small nonelectrolyte solutes (i.e., the "iceberg formation") is still correct. However, the hydrogen-bond probability of bulk H_2O away from solutes is reduced progressively, as the solute composition increases. When the hydrogen-bond probability of bulk H_2O is reduced to the bond percolation threshold of the hexagonal ice connectivity, the hydrogen-bond percolation is lost and a qualitatively different mixing scheme sets in, whereby the solution consists of two kinds of clusters. In the solute-rich region, solute molecules form clusters of its own kind. Thus, the "iceberg formation" is basically correct within a narrow range in the H_2O-rich region for small nonelectrolyte solutes. Thus, reference made to the "iceberg" concept in recent literatures should be clarified in terms of the concentration range and the size of solute in question.

Introduction

For the last half a century, the concept of "iceberg formation"[1] has played an important role in understanding the nature of aqueous solutions of a variety of nonelectrolytes.[2−4] The original concept,[1] however, was formulated using the partial molar entropy at infinite dilution data available at the time (1945). It is therefore applicable only in dilute aqueous solutions. Nonetheless, this concept has been taken overly seriously, and each time an experimental observation is made contrary to this concept, it has been criticized or challenged, irrespective of the concentration of solute nonelectrolyte.[5] Another confusion arises from the size of hydrophobic moiety in question. The original suggestion was based on the data for nonelectrolytes of molecular weight about 100 at most. Thus, application of this concept for function and structure of macromolecules, including biopolymers, is an overinterpretation. Indeed, there is a theoretical work suggesting that the "iceberg" concept is applicable for small hydrophobic moieties. For moieties with large surface areas and curvatures, the hydrogen bonds of H_2O are broken at all temperatures.[6] For aqueous lysozyme, a combination of X-ray and neutron-scattering study suggests that the first hydration shell has an average density about 10% higher than bulk H_2O,[7] hinting no "icebergs". We note, however, that lysozyme under the conditions of this study is in the native form and that 39% of the outer surface is covered by hydrophilic moieties.[8] For flat hydrophobic surfaces, vibrational studies that probe molecular structure at CCl_4/H_2O, and hydrocarbon/H_2O interfaces showed that the hydrogen bonding between adjacent H_2O molecules is weak.[9] An X-ray reflectivity measurement on H_2O/paraffin interfaces indicated depletion of H_2O density, i.e., so-called dewetting.[10] An atomic force microscopy revealed an extreme depletion to the point of formation of "nanobubbles" on flat hydrophobic surfaces.[11] On the other hand, a molecular dynamic simulation study of H_2O confined in carbon nanotubes narrower than the critical diameter could be in a state having an ice-like mobility with an amount of hydrogen bonding similar to that of liquid H_2O.[12] The present status of studies on H_2O in the vicinity of flat hydrophobic surfaces is tersely reviewed recently.[13] Thus, the iceberg concept appears to be in turmoil at present, which we believe could be sorted out by clarifying the conditions under which consideration is given.

Here we limit our attention to small nonelectrolytes, monools in particular, and defend the concept of "iceberg" formation in the H_2O-rich region by reviewing our recent findings using the methodology in solution thermodynamics introduced by us.

Our Methodology of Solution Thermodynamics

Since 1986,[14] we have started a methodology in solution thermodynamics, on which detailed review articles are available.[15−17] A brief account is given here. Primary thermodynamic quantities in solution systems that are conventionally determined are H^E, S^E, and V^E, all of which contain a first-order derivative of Gibbs energy, G. H^E, for example, is the excess enthalpy of a solution as a whole. Although H^E reflects nonideality resulting from enthalpic interactions among constituents, it signifies the net results of all interactions. Thus, the information gained is limited to a macroscopic average behavior. To advance a step toward molecular level understanding, we determine experimentally the excess partial molar enthalpy of solute B in aqueous solution, $H_B{}^E$, which is defined as

$$H_B{}^E \equiv (\partial H^E/\partial n_B) \qquad (1)$$

keeping other independent variables, n_W, p, and T, constant. n_B and n_W are the amount of B and solvent W(H_2O), in the system

* Author to whom correspondence may be addressed. E-mail: koga@chem.ubc.ca. Fax: (604) 822-2847. Phone: (604) 822-3491.
† The University of British Columbia.
‡ Roskilde University.
§ Chiba University.

10.1021/jp0312722 CCC: $27.50
Published on Web 04/02/2004

with the total amount $N = n_B + n_W$. In practice, we titrate a small amount of B, δn_B, and measure the enthalpic response in H^E, δH^E. We then approximate the quotient $\delta H^E/\delta n_B$ to $H_B{}^E$, eq 1. The goodness of the approximation is checked by reducing the size of δn_B and seeing the quotient to converge. Since H^E contains the first-order derivative of the Gibbs energy, G, $H_B{}^E$ represents a second derivative. As its definition, eq 1, implies, $H_B{}^E$ is the actual contribution of solute B in terms of enthalpy of the entire system. Hence it provides the information about B's actual enthalpic situation in the solution, which is clearly more detailed than H^E.

We determine $H_B{}^E$ accurately and in small increments in composition, and we can take one more compositional derivative graphically without resorting to a fitting function. Thus we obtain purely experimentally the third derivative quantity $H_{B-B}{}^E$ as

$$H_{B-B}{}^E \equiv N(\partial H_B{}^E/\partial n_B) = (1 - x_B)(\partial H_B{}^E/\partial x_B) \qquad (2)$$

where x_B is the mole fraction of B. We call $H_{B-B}{}^E$ the B−B enthalpic interaction function, since it signifies the effect of additional B on the actual enthalpic situation of B in the mixture. Thus, $H_{B-B}{}^E$ provides a measure of the B−B interaction in terms of enthalpy and contains in turn more detailed information than $H_B{}^E$. Analogous quantities to eq 2 can also be obtained for entropy, $S_{B-B}{}^E$, and volume, $V_{B-B}{}^E$. We emphasize that these interaction functions are obtained purely experimentally and completely model free. According to thermodynamic stability criteria, the sign of $H_{B-B}{}^E$ or $S_{B-B}{}^E$ can indicate that the B−B interaction is favorable or not.

We have used these and other second- and third-order derivatives of G and revisited aqueous solutions of nonelectrolytes.[15−17] We summarize our findings below. The more detailed account has been given elsewhere.[15−17]

Mixing Schemes in Aqueous 2-Butoxyethanol. We show our findings for aqueous 2-butoxyethanol (BE). This solute contains the largest hydrophobic moiety that we have studied, but may still be small enough (MW 118) to fall in the group that was considered by Frank and Evans.[1] Furthermore, BE is probably the largest mono-ol miscible with H_2O in the entire composition range at about the room temperature, although the liquid−liquid-phase separation occurs above 50 °C, the lower critical solution temperature (LCST).

Figure 1 shows the plots of $H_{BE}{}^E$ and $TS_{BE}{}^E$ against x_{BE}.[15−17] Note that the product $TS_{BE}{}^E$ is used and the units are the same with $H_{BE}{}^E$. x_{BE} is the mole fraction of BE. Conspicuous changes in the x_{BE} dependence in Figure 1 immediately suggest that there are three regions approximately bound by arrows in the figure, in each of which the thermodynamic behavior and hence the mixing scheme, or the solution structure, is qualitatively different from other regions. The excess partial molar enthalpy and entropy of H_2O, $H_W{}^E$, and $TS_W{}^E$, are plotted in Figure 2. They are related to $H_{BE}{}^E$ and $TS_{BE}{}^E$ via the Gibbs−Duhem relation.

In the most BE-rich region, the zero values of $H_{BE}{}^E$ and $S_{BE}{}^E$ suggest that BE molecules in the mixture is in the same environment locally as in the pure state, and hence they must exist as clusters, perhaps in a micellar form. H_2O molecules, on the other hand, seem to interact with BE clusters as a single molecule, since $H_W{}^E$ stays constant and $S_W{}^E$ is almost constant in this composition region. We call this mode of mixing mixing scheme III. For aqueous solutions of other smaller alcohols (AL), AL molecules also tend to cluster together with their own kinds in the AL-rich region. However, how H_2O molecules interact with AL clusters depends strongly on the individual characteristics of AL. The details of mixing scheme III for other alcohols are under investigation.

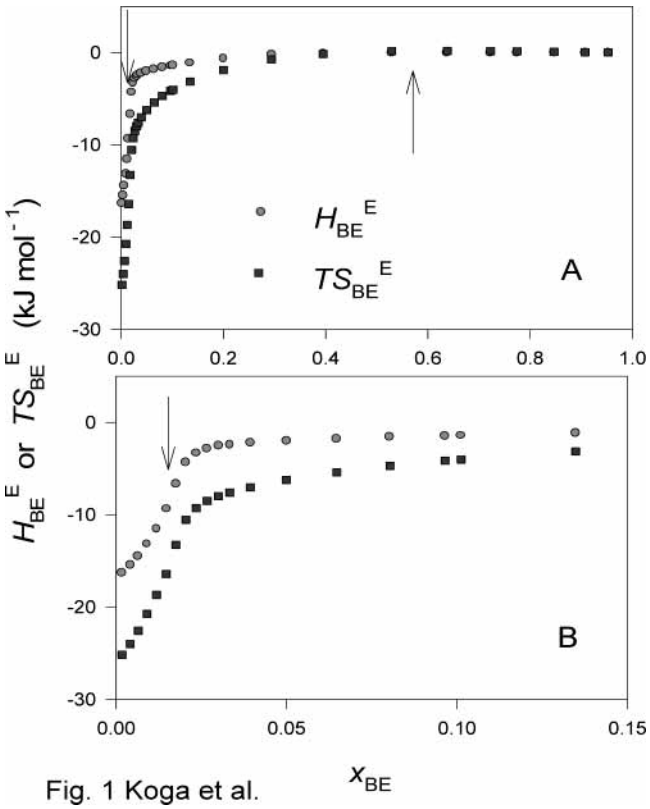

Figure 1. Excess partial molar enthalpy and entropy of BE, $H_{BE}{}^E$ and $TS_{BE}{}^E$, against mole fraction of BE, x_{BE}, at 25 °C. (●) $H_{BE}{}^E$; (■) $TS_{BE}{}^E$. The arrows indicate probable loci where change over occurs in mixing scheme.

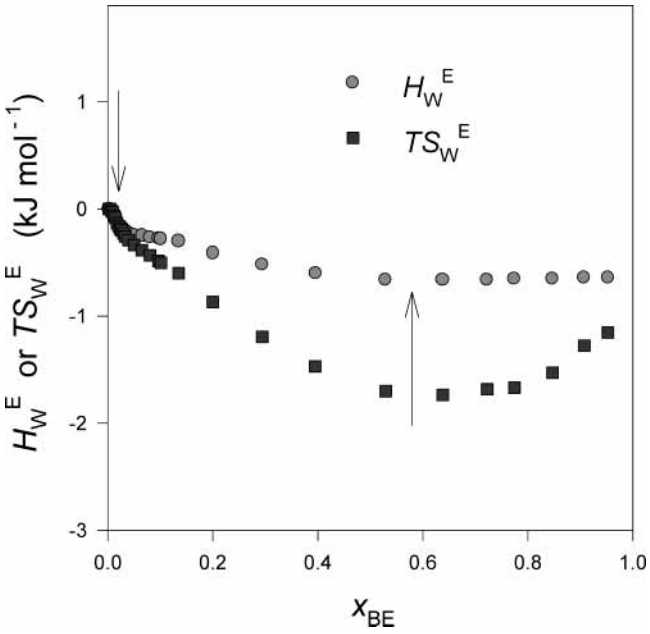

Figure 2. Excess partial molar enthalpy and entropy of H_2O, $H_W{}^E$ and $TS_W{}^E$, against x_{BE} at 25 °C. (●) $H_W{}^E$; (■) $TS_W{}^E$.

In the intermediate region, BE−H_2O phase separates with the LCST at 50 °C and $x_{BE} = 0.06$.[18] At 25 °C, therefore, this composition region is supercritical. Indeed, the intensities of light scattering[19] and small-angle X-ray scattering[20] increase sharply near the LCST, indicating existence of clusters. Furthermore, the fact that $H_{BE}{}^E$ and $S_{BE}{}^E$ have positive slopes as

x_{BE} increases (i.e., $H_{BE-BE}^{E} > 0$ and $S_{BE-BE}^{E} > 0$) in this region is consistent for the system having phase separation with an LCST.[15,16] Intuitively, $H_{B-B}^{E} > 0$ drives B and W to mix and $S_{B-B}^{E} > 0$ to unmix. Since $G = H - TS$ dictates the fate of an equilibrium system, the entropy contribution is more dominant at higher temperatures, and hence the enthalpy effect is important at lower temperatures. At higher temperatures than 50 °C, B and W unmix because $S_{B-B}^{E} > 0$, while at lower temperatures, they mix because $H_{B-B}^{E} > 0$. More detailed arguments on this have been given elsewhere[15,16] and in a reference cited therein. Thus, we conclude that BE−H_2O in this composition range consists of two kinds of clusters, one rich in H_2O and the other in BE. These clusters grow in size to a macroscopic scale when temperature is raised above the LCST. We call this mixing scheme II.

For other smaller alcohols, sharp increases in scattering intensities were also observed,[21−23] although there is no apparent phase separation before vaporization occurs. The signs of H_{B-B}^{E} and S_{B-B}^{E} are also positive in this region for all the mono-ol cases studied.[15−17,24] We conclude that the same mixing scheme is operative for other alcohols. In these systems, an LCST might be hidden above the vaporization temperature.

The H_2O-Rich Region of Aqueous BE. We now turn to the H_2O-rich region, where the "iceberg" concept is originally formulated.[1] As shown in Figure 1B, a small amount of BE is introduced into H_2O with a large enthalpy gain, −17 kJ mol^{-1}, and a larger entropy loss, −26 kJ mol^{-1}. This magnitude is only discernible if we consider some effect of BE on the molecular organization of solvent H_2O, in particular, the "iceberg" formation induced by BE. An isotope effect of H_{BE}^{E} clearly indicated that it is the solvent (H_2O or D_2O) that affects the value of H_{BE}^{E}, while there was no effect by changing −OH to −OD in BE in this composition range.[25] It is also striking that the thermodynamic situation is rapidly changing as x_{BE} increases. In the first place, Figure 1 shows that the absolute value of H_{BE}^{E} is progressively decreasing and exerting lesser effect as more BE is added. This suggests that the effect of BE is of a long range. Since the first BE has already made some changes in H_2O, the second BE exerts lesser effects. When such a process completes its course and reaches the threshold, mixing scheme II sets in. At first sight, therefore, the iceberg formation may be complete at about the locus of the arrow in Figure 1B, and there is no room for further accommodation of BE in the same manner. BE molecules are then forced to cluster together, pertinent to the BE-rich clusters in mixing scheme II discussed above. This may hint that the aqueous part of the system consists entirely of icebergs at the boundary. If so, the ionic conductivity of H^+ and OH^- is expected to increase in BE−H_2O as x_{BE} increases to the boundary due to proton hopping along the completed hydrogen bond network. Contrary to this expectation, the ionic conductivity in fact decreased.[26] This was the first hint that the iceberg does not fill the entire system but rather the hydrogen bond probability of bulk H_2O away from icebergs may in fact be decreasing. This issue will be discussed throughout the remainder of this section.

Figure 3 shows the excess partial molar volume of BE, V_B^{E}, and that of H_2O, V_W^{E}.[27,28] If the entire system is filled with iceberg at the boundary, the value of V_W^{E} would be close to that for ice, about 1.5 cm^3 mol^{-1}! Figure 3B indicates a small increase in V_W^{E}, hinting iceberg formation, but the increase is some thousandths of the above value. There must therefore be an additional mechanism operating to reduce V_W^{E} progressively as x_{BE} increases.

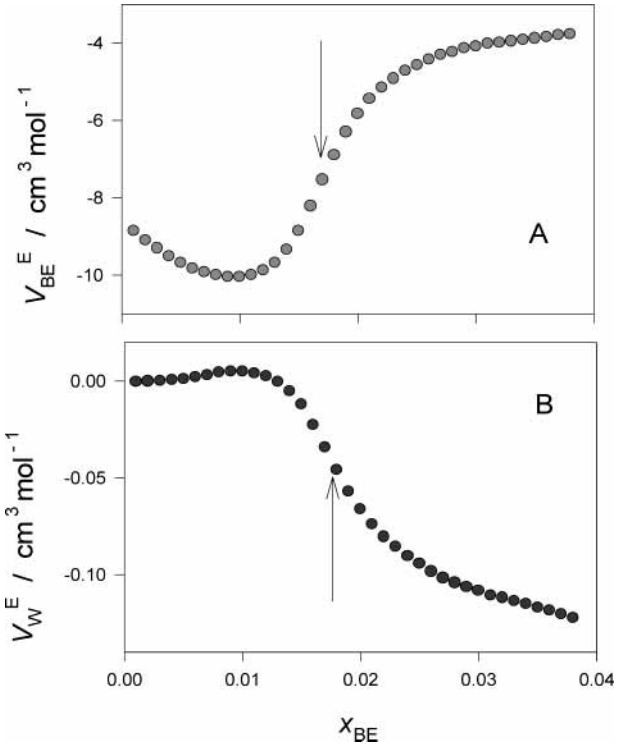

Figure 3. (A) Excess partial molar volume of BE, V_{BE}^{E}, against x_{BE} at 25 °C. (B) Excess partial molar volume of H_2O, V_W^{E}, against x_{BE} at 25 °C.

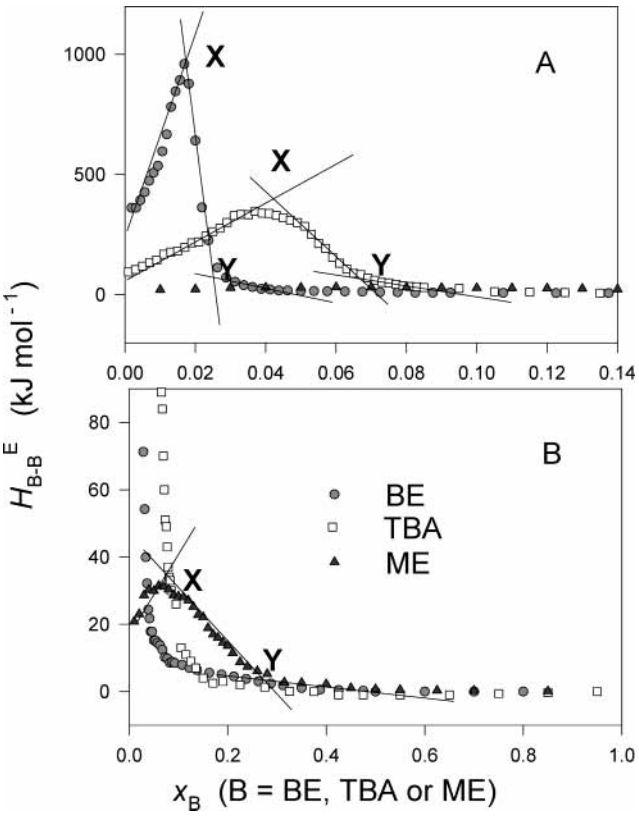

Figure 4. Enthalpic interaction function, H_{B-B}^{E}, for B = BE, TBA, or ME against mole fraction x_B at 25 °C. (●) BE; (■) TBA; (▲) ME.

Before settling this issue, we turn to the third-derivative quantities. The enthalpic interaction, H_{BE-BE}^{E}, eq 6, for BE−H_2O is shown in Figure 4. The entropic interactions are almost identical to H_{BE-BE}^{E} [15−17] because of the entropy−enthalpy compensation effect. In Figure 4, the equivalent data, H_{B-B}^{E},

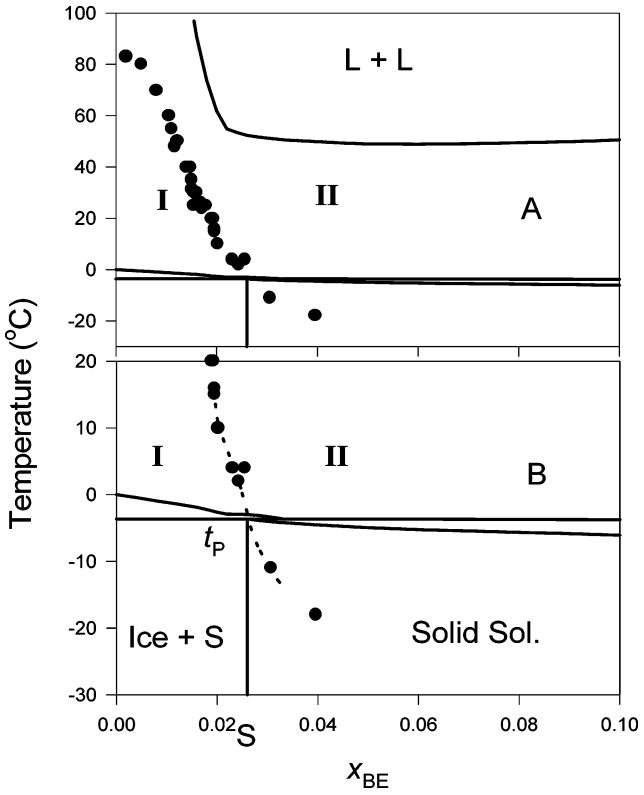

Figure 5. Mixing-scheme diagram for BE−H_2O. S is an addition compound $BE(H_2O)_{38}$. t_P is the incongruent melting point of S. I and II signify the regions of mixing schemes I and II, respectively.

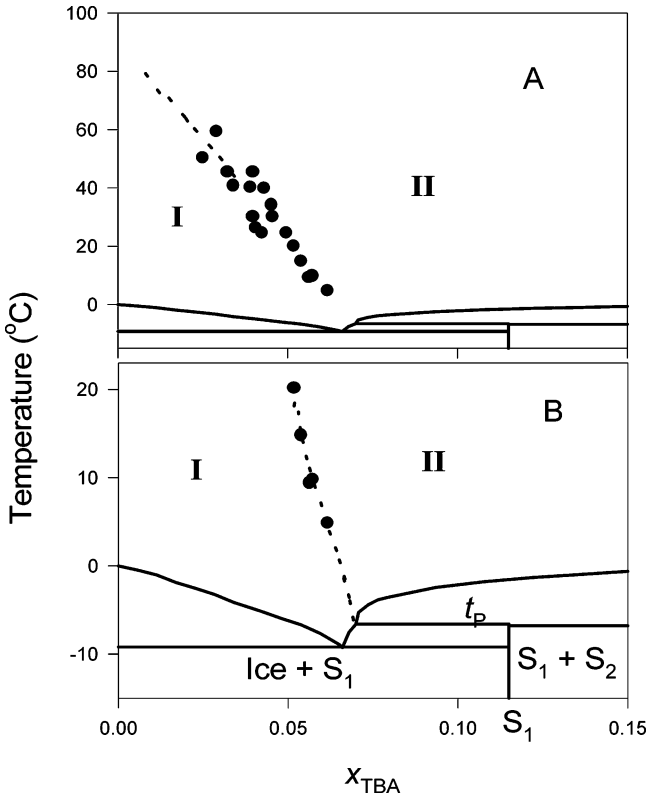

Figure 6. Mixing-scheme diagram for TBA−H_2O. S_1 is an addition compound $TBA(H_2O)_m$. See text for m. t_P is the incongruent melting point of S_1. S_2 is $TBA(H_2O)_2$. I and II signify the regions of mixing schemes I and II, respectively.

are also shown for aqueous methanol (ME) and aqueous *tert*-butyl alcohol (TBA), i.e., for B = TBA or ME. As is evident from the figure, these alcohols behave in a similar manner in this region even in the third derivative quantities. Indeed, all the other H_2O-miscible mono-ols we have studied, ethanol and 1- and 2-propanol, have qualitatively similar thermodynamic behaviors. It is the size of hydrophobic moiety that makes quantitative variations, and its effect is stronger for a larger size in terms of the value of H_{B-B}^E. A larger hydrophobic moiety also requires a lesser amount of solute to drive the mixture to the boundary to mixing scheme II.[15−17]

The x_B dependence of H_{B-B}^E for B = BE, TBA, or ME in Figure 4 resembles anomalies in heat capacity (a second derivative of G) associated with phase transitions. "Phase" is a macroscopic entity, and its transition is accompanied by an anomaly in second-order derivatives of G. In contrast, the present transition from mixing schemes I to II is more subtle and associated with anomalies in third derivatives. Figure 3 shows that the boundary at $x_{BE} = 0.017$ corresponds also to the inflection point of V_{BE}^E, and hence $V_{BE-BE}^E \equiv N(\partial V_{BE}^E/\partial n_{BE})$ will show the maximum at this point.[28] While we learn from Figure 4 that the boundary between mixing schemes I and II should actually be a boundary region denoted as X and Y in the figure,[17] we collected the loci of the maxima (point X) in various third derivatives and plotted them in Figure 5, together with the phase diagram.[18] See review articles[15−17] for details about a variety of third derivatives and types of their anomalies. These plots seem to form a single line, sometimes called the "Koga line",[17] which seems to cut the ordinate at about 85 °C. We recall the site-correlated percolation model for liquid H_2O by Stanley et al.,[29] in which the hydrogen bond network is understood to be bond percolated at about room temperature, with the observation that the water oxygens with four hydrogen bonds tend naturally to cluster together, resulting in the so-called "ice-like patches". In the appendix of ref 29, the authors gave an estimate of the global average of hydrogen-bond probability as a function of temperature. This estimate shows the hydrogen-bond probability reaches 0.39, the bond percolation threshold for the hexagonal ice-type connectivity[30] at about 85 °C. This coincidence of 85 °C may suggest that the boundary line shown in Figure 5 is in fact the hydrogen-bond percolation threshold for a bulk H_2O in solution. Namely, mixing scheme I is such that the hydrogen-bond network of H_2O is enhanced in the vicinity of BE ("iceberg formation"), but at the same time the hydrogen-bond probability of bulk H_2O away from the "iceberg"-clad BE is progressively reduced until it reaches 0.39. Thereupon, the system loses the hydrogen-bond network and consists of two kinds of clusters.

Prior to this threshold, the balance of the hydrogen bond enhancement in the vicinity of BE and the concomitant reduction of the hydrogen-bond probability of bulk H_2O away from BE dictates the x_{BE} dependence of H_B^E and S_B^E in mixing scheme I, Figure 1. A very small increase in V_W^E, Figure 3B, is thus the result of this balance between an increase due to "iceberg" and a decrease by reduced hydrogen-bond probability of bulk H_2O. The initial decrease in V_{BE}^E, Figure 3A, is of course the consequence of the Gibbs−Duhem relation. Its molecular level interpretation can be given as follows. The negative value of V_{BE}^E at the infinite dilution is caused primarily by the "sand-and-pebble" effect. However, H_2O is a bulky "sand" due to hydrogen bonds, which give a positive contribution to the net result. As x_{BE} increases, this positive contribution decreases, and hence V_B^E decreases, since the hydrogen bond probability of bulk H_2O and bulkiness of the "sand" is progressively reduced. Thus, the decrease in ionic conduction in BE−H_2O mentioned above was due to the reduction of the hydrogen-

bond probability of bulk H_2O, through which ionic conduction takes place.

Another notable feature in Figure 5 is that the mixing-scheme boundary ends at the incongruent melting point of an addition compound, $BE(H_2O)_{38}$ (a clathrate?).[18] This suggests that mixing scheme I is preparing for the formation of the addition compound on freezing, which provides another circumstantial evidence for "icebergs" in solution. On cooling BE−H_2O in mixing scheme I, ice separates out at the liquidus curve and eventually the addition compound $BE(H_2O)_{38}$ forms. Since the hydrogen-bond probability of bulk H_2O is reduced due to the presence of BE, the system requires a lower temperature than 0 °C to form ice, a molecular level understanding of the freezing point depression normally deduced by thermodynamic reasoning.

Aqueous TBA in the H_2O-Rich Region. Figure 6 is the mixing scheme[15−17] and phase[31−33] diagram for TBA−H_2O. Just like BE−H_2O, the mixing-scheme boundary seems to cut the ordinate at about 85 °C. At present, the mixing-scheme diagrams for aqueous solutions of other alcohols are not available. The only other example is for aqueous acetonitrile.[17] This boundary also seems to point to 85 °C at the ordinate.[17] Turning back to TBA−H_2O, the extension of the boundary to lower temperatures in Figure 6 appears to point toward the intersection of the liquidus curve and the incongruent melting point of an addition compound, $TBA(H_2O)_m$. The value of *m* is still controversial. The values of 6,[31] 7,[32] and 7.7[33] were suggested for *m*. In any case, the fact that an addition compound and ice form on cooling TBA−H_2O in this region could also serve to support the "iceberg formation" in mixing scheme 1.

Conclusion

Though not explicitly stated, the original idea of "iceberg formation" was meant to be applicable in the infinite dilution of aqueous solutions of small nonelectrolytes.[1] As discussed above, we have modified the concept a little and clarified the applicable range. The mole fractions of point X, the onset of the transition to mixing scheme II, are 0.017 for BE, 0.045 for TBA, and 0.07 for ME, at room temperature. The available loci of the boundary are listed for all the nonelectrolytes we have studied so far.[17] Thus, the applicable concentration range is still narrow in the H_2O-rich region. Hence, the desirable structural investigations must be aimed at these narrow dilute concentration regions. There are indeed some examples of spectroscopic and scattering studies in mixing scheme I regions, with mixed conclusions; some support the "iceberg" concept, while others do not. A dynamic light-scattering study indicated a sharp decrease in the size of diffusing species at the boundary from mixing schemes I to II in BE−H_2O.[34] An NMR study showed a sudden increase in the degree of self-association of TBA.[35] In another NMR and IR study,[36] although an initial increase in a proton chemical shift turns around at about the boundary for TBA−H_2O, no direct evidence was available for "iceberg formation". Neutron-scattering studies on ME−H_2O[37] and TBA−H_2O[38] in the respective mixing scheme I region suggest no structural difference from that in the alcohol-rich regions and hence reject the "iceberg" concept.[5] Spectroscopy and scattering techniques, though aiming at direct structural elucidation at the molecular level, provide the information of a global average. As described above, the "iceberg formation" is a local enhancement with concomitant reduction of hydrogen-bond probability away from solutes. Thus, a new technique to probe an immediate vicinity of a hydrophobic solute of small size is awaited. For flat surfaces, a few techniques are apparently available, as mentioned in the Introduction, pending, however, the fact that the so-called "flat" interfaces between two phases, H_2O and an organic liquid, are surely not flat at the molecular level. Furthermore, there may be mutual dissolution across the interface of two phases.

Acknowledgment. We thank many students for their work toward this paper. We also acknowledge general financial support by NSERC of Canada, the Ministry of Education, Science and Culture, Japan, and the Danish National Research Council throughout this work.

References and Notes

(1) Frank, H. S.; Evans, M. W. *J. Chem. Phys.* **1945**, *13*, 507.
(2) Franks, F.; Ives, D. J. G. *Q. Rev.* **1966**, *20*, 1.
(3) Franks, F.; Desnoyers, J. E. In *Water Science Reviews*; Franks, F., Ed.; Cambridge University Press: New York, 1985; Vol. 1, pp 171−232.
(4) *Water: A Comprehensive Treatise*; Franks, F., Ed.; Plenum: New York, 1972−1982; Vols. 1−7.
(5) Dixit, S.; Crain, J.; Poon, W. C. K.; Finney, J. L.; Soper, A. K. *Nature* **2002**, *416*, 829.
(6) Southall, N. T.; Dill, K. A. *J. Phys. Chem. B* **2000**, *104*, 1326.
(7) Svergun, D. I.; Richard, S.; Koch, M. H. J.; Sayers, Z.; Zaccai, G. *Proc. Natl. Acad. Sci. U. S. A.* **1998**, *95*, 2267.
(8) Makhatadze, G. I.; Privalov, P. L. *Adv. Protein Chem.* **1995**, *47*, 307.
(9) Scatina, L. F.; Brown, M. G.; Richmond, G. L. *Science* **2001**, *292*, 908.
(10) Jensen, T. R.; Jensen, M. O.; Reitzel, N.; Balashev, K.; Peters, G. H.; Kjaer, K.; T. Bjornholm, T. *Phys. Rev. Lett.* **2003**, *90*, 086101.
(11) Tyrrell, J. W.; Attard, P. *Phys. Rev. Lett.* **2001**, *87*, 176104.
(12) Mashl, J.; Joseph, S.; Aluru, N. R.; Jakobsson, E. *Nano Lett.* **2003**, *3*, 589.
(13) Ball, P. *Nature* **2003**, *423*, 25.
(14) Koga, Y. *Can. J. Chem.* **1986**, *64*, 206.
(15) Koga, Y. *J. Crys. Soc. Jpn.* **1995**, *37*, 172.
(16) Koga, Y. *J. Phys. Chem.* **1996**, *100*, 5172.
(17) Koga, Y. *Netsu Sokutei* **2003**, *30*, 54. (Available in a PDF form on request to the author).
(18) Koga, Y.; Tanaka, T.; Atake, T.; Westh, P.; Hvidt, Aa. *Bull. Chem. Soc. Jpn.* **1994**, *67*, 2393.
(19) Ito, N.; Fujiyama, T.; Udagawa, Y. *Bull. Chem. Soc. Jpn.* **1983**, *56*, 379.
(20) Hayashi, H.; Udagawa, Y. *Bull. Chem. Soc. Jpn.* **1992**, *65*, 600.
(21) Koga, Y. *Chem. Phys. Lett.* **1984**, *111*, 176.
(22) Nishikawa, K.; Hayashi, H.; Iijima, T. *J. Phys. Chem.* **1989**, *93*, 6559.
(23) Nishikawa, K.; Iijima, T. *J. Phys. Chem.* **1993**, *97*, 10824.
(24) Koga, Y.; Westh, P.; Nishikawa, K. *Can. J. Chem.* **2003**, *81*, 150.
(25) Siu, W. W. Y.; Wong, T. Y. H.; Lai, J. T.; Chong, A.; Koga, Y. *J. Chem. Thermodyn.* **1992**, *24*, 159.
(26) Koga, Y.; Loo, V. L.; Puhacz, K. T. *Can. J. Chem.* **1995**, *73*, 1294.
(27) Koga, Y.; Kristiansen, J.; Hvidt, Aa. *J. Chem. Thermodyn.* **1993**, *25*, 51.
(28) Koga, Y. *J. Phys. Chem.* **1992**, *96*, 10466.
(29) Stanley, H. E.; Teixeira, J. *J. Chem. Phys.* **1980**, *73*, 3044.
(30) Parsonage, N. G.; Staveley, L. A. K. *Disorder in Crystals*; Clarendon Press.: Oxford, 1978; p 84.
(31) Ott, J. B.; Goates, J. R.; Waite, B. A. *J. Chem. Thermodyn.* **1979**, *11*, 739.
(32) Mootz, D.; Staeben, D. *Z. Naturforsch. B: Chem. Sci.* **1993,** *48*, 1325.
(33) Takaizumi, K. *J. Solution Chem.* **2000**, ***29***, 377.
(34) Bender, T. M.; Pecora, R. *J. Phys. Chem.* **1988**, *92*, 1675.
(35) Mayele, M.; Holz, M.; Secco, A. *Phys. Chem. Chem. Phys.* **1999**, *1*, 4515.
(36) Mizuno, K.; Kimura, Y.; Morichika, H.; Nishimura, Y.; Shimada, S.; Maeda, S.; Imafuji, S.; Ochi, T. *J. Mol. Liq.* **2000**, *85*, 139.
(37) Dixit, D.; Soper, A. K.; Finney, J. L.; Crain, J. *Euro. Phys. Lett.* **2002**, *59*, 377.
(38) Bowron, D. T.; Finney, J. L. *J. Chem. Phys.* **2003**, *118*, 8357.